

ASITP

INSTITUTE OF THEORETICAL PHYSICS

ACADEMIA SINICA

AS-ITP-96-07

March 1996

Difference in moments of inertia and pairing
interaction strength in the superdeformed Hg nuclei

Y. A. Lei, T. H. Jin, J. Y. Zeng

5w9637

SCAN-9609009



CERN LIBRARIES, GENEVA

P.O.Box 2735, Beijing 100080, The People's Republic of China

Telefax : (86)-10-2562587

Telephone : 2568348

Telex : 22040 BAOAS CN

Cable : 6158

Difference in moments of inertia and pairing interaction strength in the superdeformed Hg nuclei

Y. A. Lei^{a,b,c}, T. H. Jin^b, J. Y. Zeng^{a,b,c}

^aChina Center of Advanced Science and Technology (World Laboratory),
Center of Theoretical Physics, P. O. Box 8730, Beijing 100080

^bDepartment of Physics, Peking University, Beijing 100871

^cInstitute of Theoretical Physics, Chinese Academy of Sciences, Beijing 100080

Abstract

The difference in the bandhead moments of inertia between the yrast superdeformed (SD) band $^{194}\text{Hg}(1)$ and the two-quasiparticle SD bands $^{194}\text{Hg}(2,3)$ was investigated using the particle-number-conserving treatment for the cranked shell model Hamiltonian, and the pairing interaction strength in SD nuclei is estimated to be much weaker than that in normally deformed nuclei.

PACS numbers: 21.10Re, 27.70+q, 21.60-n.

1 Introduction

Since the discovery of the superdeformed (SD) band ^{191}Hg (yrast) [1], an impressive experimental and theoretical effort has been devoted to exploring the underlying physics of SD bands in the mass $A \sim 190$ region. To date, about fifty SD bands in 17 nuclei have been reported in this mass region. A striking difference between the SD bands near $A = 190$ and those in the other regions is that the vast majority SD bands near $A = 190$ display the similar rise in the dynamic moment of inertia $J^{(2)}$ as a function of rotational frequency [2] (\sim an increase of 30–40 % over the frequency $\hbar\omega \sim 0.1\text{--}0.4$ MeV), which is ascribed to the successive alignment of neutrons and protons in the presence of pairing correlation [3–5]. Calculations with no pairing correlation give essentially no frequency dependence of $J^{(2)}$, so the inclusion of pairing is crucial for reproducing the smooth increase of $J^{(2)}$ with frequency.

On the other hand, it has been well known that for the ground bands of normally deformed (ND) nuclei, the rise in $J^{(2)}$ (below bandcrossing) with frequency is much steeper than that in SD nuclei. For example, for the ground band of ^{238}U , the bandhead moment of inertia is about $J^{(2)}(\omega = 0) \approx 70\hbar^2\text{MeV}^{-1}$, but $J^{(2)}(\omega \approx 0.25\text{MeV}) \approx 210\hbar^2\text{MeV}^{-1}$, i.e., there is an increase of about 200 % over the frequency range $\hbar\omega \sim 0\text{--}0.25$ MeV. This may be considered as an evidence that the pairing interaction strength in SD nuclei near $A = 190$ may be much weaker than that in ND nuclei.

Another striking feature of the SD bands is that the transition energies of many SD bands are almost identical [6]. Since pair correlations play an important role in the $A = 190$ SD nuclei as mentioned above, the observation of so many bands in even and odd mass nuclei with similar moments of inertia is surprising. Of course, it should be noted that the “identity” of some SD bands was established only within certain frequency range; e.g., the excited SD bands $^{194}\text{Hg}(2,3)$ are identical to the yrast SD band $^{192}\text{Hg}(1)$ only within the frequency range $\hbar\omega \approx 0.20\text{--}0.40$ MeV, but at lower frequencies ($\hbar\omega \sim 0.1\text{--}0.2$ MeV) the moments of inertia of $^{194}\text{Hg}(2,3)$ are systematically larger than that of $^{192}\text{Hg}(1)$ (see also Figs. 1 and 2). Similarly, the $J^{(2)}$'s of the yrast SD band $^{194}\text{Hg}(1)$ at lower frequencies are systematically smaller than those of the excited bands $^{194}\text{Hg}(2,3)$, which have been ascribed to the two-quasiparticle excitation ($[512]5/2 + [624]5/2$) [3]. In this paper, we will show that the differences in the moments of inertia in SD nuclei at low frequencies may be considered as another evidence of pairing interaction in SD nuclei, and valuable information on the pairing interaction strength may be extracted from these observed differences.

As has been pointed out by Chasman [7] that the single-particle level density near the

Fermi surface of a SD nuclei is small, which means that the pairing correlation energy is weak. He also emphasized that a BCS treatment of pairing is not correct in this limit, hence is not appropriate for SD states.

Moreover, in a previous paper [8] for treating the microscopic mechanism of the odd-even difference in the moments of inertia of ND nuclei, it has been demonstrated that this difference is crucially connected with the proper treatment of blocking effect. In fact, all the odd-even differences in various properties of nuclei are originated from the blocking effect on pairing. Liang et al. [9], found that the dynamic moments of inertia $J^{(2)}$ of two SD bands in ^{192}Tl are almost constant with the rotational frequency $\hbar\omega$, and pointed out that this constancy may be understood in terms of the blocking of low- Ω intruder orbits by both the odd proton and the odd neutron (double blocking). Later, two SD bands in ^{193}Pb [10] and in ^{195}Pb [11], whose dynamic moments of inertia are nearly constant as a function of $\hbar\omega$, were reported, which was also considered as an evidence of the blocking of $N = 7$ intruder orbits. As Rowe emphasized [12], while the blocking effect are straightforward, it is very difficult to treat them in the BCS formalism, because they introduce different quasiparticle bases for different blocked levels.

In the present paper, to account for the differences in the moments of inertia between the yrast SD (quasiparticle vacuum) band $^{194}\text{Hg}(1)$ and the excited (two-quasiparticle) SD bands $^{194}\text{Hg}(2,3)$, we adopt the particle-number-conserving (PNC) treatment [13,8] for the eigenvalue problem of the cranked shell model (CSM) Hamiltonian, in which the blocking effects are treated exactly and the number of particle are conserved from beginning to end. For convenience, a sketch of this PNC formalism is given in Sect. III A, and the calculated results and discussions are given in Sect III B and C. Before this microscopic calculation, in Sect. II we will give a brief review of the phenomenological analysis of the SD bands in $^{192,194}\text{Hg}$ to extract some reliable informations on their moments of inertia.

2 Brief review of a phenomenological analysis of the SD bands $^{192}\text{Hg}(1)$ and $^{194}\text{Hg}(1,2,3)$

The γ transition energies in the yrast SD band $^{192}\text{Hg}(1)$ have been reported in a series of papers by Becker et al. [14], Ye et al. [4], Janssens et al. [2] Lauritsen et al. [15], Gall et al. [16] and Fallon et al. [5]. The yrast SD band $^{194}\text{Hg}(1)$ and excited SD bands $^{194}\text{Hg}(2,3)$ were reported in papers by Riley et al. [3], Beausang et al. [17], Cullen et al. [18] and Cederwall et al. [19]. Because the spins of the levels in each SD band has not been observed directly

in the experiment, usually only the dynamic moment of inertia $J^{(2)}(I) = 4\hbar^2/\Delta E_\gamma(I) = 4\hbar^2/[E_\gamma(I+2 \rightarrow I) - E_\gamma(I \rightarrow I-2)]$ is addressed. There have been several approaches to address the spin assignment of SD bands [20–23]. The spin assignment of the SD band $^{192}\text{Hg}(1)$ has been given in the papers by Becker et al. [20], Ye et al. [4], Janssens et al. [2], Stephens et al. [6] and refs. [21–23]. The spin assignments of the SD bands $^{194}\text{Hg}(1,2,3)$ have been given in the papers by Beausang et al. [17], Cullen et al. [18], Stephens et al. [6] and refs. [20–23]. It is noted that the spin assignments for the SD bands $^{192}\text{Hg}(1)$ and $^{194}\text{Hg}(1,2,3)$ are consistent with each other in these papers. Though some comments on the uncertainty of these spin assignments were raised [24], considering the spins of the lowest levels observed in these SD bands are rather low, in this paper we assume that the spin assignments (see Table 1) made in these papers are correct. Instead of the usually adopted Harris 3-parameter expression of the rotational spectrum and moment of inertia [20], in this paper we use a more convenient and accurate expression for the rotational spectrum, i.e., the *abc* expression [25]

$$E(I) = a \left[\sqrt{1 + bI(I+1)} - 1 \right] + cI(I+1). \quad (1)$$

Putting $c = 0$, the *abc* expression is reduced to the *ab* expression, which was suggested empirically by Holmberg and Lipas [26] and was derived from the Bohr Hamiltonian for a well deformed nucleus with small axis asymmetry ($\sin^2 3\gamma \ll 1$) [27]. The last term on the right side of (1) is introduced by considering the effect (to the first order perturbation) of higher order ($k\beta^4$) term in the potential energy of Bohr Hamiltonian. The last term is a small correction ($|c| \ll a$) and c may be positive or negative (according to the sign of k). Considering the very large quadrupole deformation and small axial asymmetry of SD nuclei, it is expected that the *abc* expression is especially suitable for the SD bands. The corresponding expressions for the kinematic and dynamic moments of inertia are

$$\frac{\hbar^2}{J^{(1)}} = \frac{ab}{[1 + bI(I+1)]^{1/2}} + 2c, \quad \frac{\hbar^2}{J^{(2)}} = \frac{ab}{[1 + bI(I+1)]^{3/2}} + 2c, \quad (2)$$

and at the bandhead both $J^{(1)}$ and $J^{(2)}$ tend to $J_0 = \hbar^2/(ab + 2c)$. It has been shown [25] that the large number of ND rotational bands in the rare-earth and actinide nuclei can be reproduced very well up to very high spin (below bandcrossing) by (1). In Table 1 the observed transition energies $E_\gamma(I) = E(I) - E(I-2)$ in the SD bands $^{192}\text{Hg}(1)$, $^{194}\text{Hg}(1)$, and $^{194}\text{Hg}(2,3)$ are used in the least squares fit to (1). It is amazing that all the E_γ 's in each SD band are reproduced unusually well with root mean square deviations $\chi < 10^{-3}$. It is well known that the transition energies E_γ 's are observed with very high

precision, but the error in their difference, $\Delta E_\gamma(I) = E_\gamma(I+2) - E_\gamma(I)$, is larger by an order of magnitude, hence the uncertainty in the dynamic moment of inertia $J^{(2)}$ extracted by $J^{(2)}(I) = 4\hbar^2/\Delta E_\gamma(I)$ is rather large. In view of the fact that the observed transition energies are reproduced so accurately by (1), it is expected that the kinematic and dynamic moments of inertia can be faithfully reproduced by the corresponding analytic expression (2). In Fig. 1 is given the comparison between the moments of inertia calculated by (2) and those extracted directly by the difference-quotient equations $J^{(1)}(I-1) = \hbar^2(2I-1)/E_\gamma(I)$ and $J^{(2)}(I) = 4\hbar^2/\Delta E_\gamma(I)$. It is seen that the $J^{(1)}$'s extracted by both approaches coincide with each other very well, but there exist some small fluctuations in the $J^{(2)}$'s extracted by $4\hbar^2/\Delta E_\gamma$ (due to the large uncertainty in ΔE_γ) around the smooth curve extracted by the analytic expression (2).

In Fig. 2(a) is plotted the ω variation of the differences in $J^{(1)}$ and $J^{(2)}$ between the SD bands $^{194}\text{Hg}(2,3)$ and $^{192}\text{Hg}(1)$. It is seen that, just as has been pointed out by Stephens et al. [6], $\delta J^{(2)} = J^{(2)}(^{194}\text{Hg}(2,3)) - J^{(2)}(^{192}\text{Hg}(1)) \approx 0$ over the frequency range $\hbar\omega = 0.2$ – 0.4 MeV, which is just the reason why $^{194}\text{Hg}(2,3)$ and $^{192}\text{Hg}(1)$ are called to be identical. However, it is obviously seen that in the frequency range $\hbar\omega = 0.1$ – 0.2 MeV and in the range $\hbar\omega < 0.1$ MeV (not yet observed), $\delta J^{(2)} > 0$. A similar plot given in Fig. 2b is for the differences in $J^{(1)}$ and $J^{(2)}$ between the excited SD bands $^{194}\text{Hg}(2,3)$ and the yrast SD band $^{194}\text{Hg}(1)$. Also it is seen that at the lower frequencies $\hbar\omega \leq 0.2$ MeV, $J^{(2)}(^{194}\text{Hg}(2,3)) > J^{(2)}(^{194}\text{Hg}(1))$. However, for the difference in the kinematic moment of inertia, both $J^{(1)}(^{194}\text{Hg}(2,3)) - J^{(1)}(^{192}\text{Hg}(1))$ and $J^{(1)}(^{194}\text{Hg}(2,3)) - J^{(1)}(^{194}\text{Hg}(1))$ are always positive, and decrease monotonically with increasing frequency. At the bandhead, both $J^{(1)}$ and $J^{(2)}$ tend to J_0 and the extracted differences in the bandhead moments of inertia are (see also Table 1)

$$\begin{aligned} J_0(^{194}\text{Hg}(2,3))|_{\text{av}} - J_0(^{194}\text{Hg}(1)) &= 5.04\hbar^2\text{MeV}^{-1} \\ J_0(^{194}\text{Hg}(1)) - J_0(^{192}\text{Hg}(1)) &= 1.60\hbar^2\text{MeV}^{-1}. \end{aligned}$$

3 Microscopic calculations and discussions

Now we make the microscopic calculation of the moments of inertia of the SD bands $^{192}\text{Hg}(1)$ and $^{194}\text{Hg}(1,2,3)$ using the PNC treatment [8,13] for the eigenvalue problem of the CSM Hamiltonian. For convenience, a sketch of the PNC formalism is given in Sect. III.A, and the calculated results (without and with pairing interaction) and discussions are given in III.B and C.

3.1 Sketch of the PNC treatment

The CSM Hamiltonian of an axially symmetric nucleus is

$$H_{CSM} = H_{SP} - \omega J_x + H_P = H_0 + H_P, \quad (3)$$

where H_{SP} is the single-particle (e.g. Nilsson) Hamiltonian, $-\omega J_x$ is the Coriolis interaction, H_P is the pairing interaction, $H_0 = H_{SP} - \omega J_x$ is the Cranked Nilsson (CN) Hamiltonian, which is a one-body operator. $H_0 = \sum_i h_0(i)$, $h_0 = h_{SP} - \omega j_x$ is for a single-particle. Let $h_0|\mu\rangle = \epsilon_\mu|\mu\rangle$, $|\mu\rangle$ is the cranked Nilsson orbit with energy eigenvalue ϵ_μ , parity π_μ and signature $r_\mu = e^{-i\pi\alpha_\mu} = \pm i$, ($\alpha_\mu = \mp 1/2$). For an n -particle system, the eigenstate $|i\rangle$ of H_0 , $H_0|i\rangle = E_i|i\rangle$, may be described by the occupation of n particles $|i\rangle = |\mu_1\mu_2\cdots\mu_n\rangle$, $E_i = \sum_{k=1}^n \epsilon_{\mu_k}$. $|i\rangle$ is called a cranked many-particle configuration (CMPC), characterized by E_i , parity π and signature $\alpha = \sum_{k=1}^n \alpha_{\mu_k}$. The eigenstate of H_{CSM} , $|\psi\rangle$, $H_{CSM}|\psi\rangle = E|\psi\rangle$, can be expressed in the CMPC space as

$$|\psi\rangle = \sum_i C_i|i\rangle. \quad (4)$$

For the yrast and low lying excited eigenstates of H_{CSM} , the accurate solution of $|\psi\rangle$ can be obtained by diagonalizing H_{CSM} in a sufficiently large CMPC space, $(E_i - E_0) < E_c$, E_0 is the energy of the lowest CMPC, $|i_0\rangle$, and E_c is sufficiently large. As in [8,13], E_c is chosen to be $0.85 \hbar\omega_0$ in the calculation, and in this case, over twenty Nilsson orbits near the Fermi surface are involved. Calculation show that all the main CMPC (weight $> 10^{-3}$) have been involved in our calculation, so the calculated low-lying eigenstates are accurate enough.

The angular momentum alignment of the state $|\psi\rangle$ is $\langle\psi|J_x|\psi\rangle$. According to the CSM, the kinematic and dynamic moment of inertia of $|\psi\rangle$ is

$$J^{(1)}(\omega) = \frac{1}{\omega} \langle\psi|J_x|\psi\rangle, \quad J^{(2)}(\omega) = \frac{d}{d\omega} \langle\psi|J_x|\psi\rangle. \quad (5)$$

Using (4), we get the expression for $J^{(1)}$

$$J^{(1)} = \frac{1}{\omega} \sum_i |C_i|^2 \langle i|J_x|i\rangle + \frac{2}{\omega} \sum_{i<j} C_i^* C_j \langle i|J_x|j\rangle, \quad (6)$$

and similar expression for $J^{(2)}$. Because J_x is a one-body operator, $\langle i|J_x|j\rangle$ is nonzero only when $|i\rangle$ and $|j\rangle$ differ by one particle occupation. Suppose that after certain permutation of creation operators, $|i\rangle$ and $|j\rangle$ are brought into the form $|i\rangle = (-)^{M_i}|\mu\cdots\rangle$, $|j\rangle = (-)^{N_j}|\nu\cdots\rangle$, where the ellipses stand for the same particle occupation and $(-)^{M_i} =$

± 1 , $(-)^{N_{j\nu}} = \pm 1$, according to the permutation is even or odd. Thus, J can be expressed in terms of the single-particle picture as

$$J^{(1)} = \frac{1}{\omega} \langle \psi | J_z | \psi \rangle = \sum_{\mu} J_{\mu\mu} + \sum_{\mu < \nu} J_{\mu\nu}, \quad (7)$$

$$\sum_{\mu} J_{\mu\mu} = \frac{1}{\omega} \sum_{\mu} \langle \mu | j_z | \mu \rangle \sum_i |C_i|^2 P_{i\mu} = \frac{1}{\omega} \sum_{\mu} \langle \mu | j_z | \mu \rangle n_{\mu}, \quad (8)$$

$$J_{\mu\nu} = \frac{2}{\omega} \langle \mu | j_z | \nu \rangle \sum_{i < j} (-)^{M_{i\mu} + N_{j\nu}} C_i^* C_j, \quad (\mu \neq \nu) \quad (9)$$

where $n_{\mu} = \sum_i |C_i|^2 P_{i\mu}$ is the particle occupation probability of the CN orbit $|\mu\rangle$ in the state $|\psi\rangle$ and $P_{i\mu} = 1$, if $|\mu\rangle$ is occupied in $|i\rangle$, and $P_{i\mu} = 0$ otherwise. If the pairing interaction is missing ($G = 0$), only one CMPC appears in $|\psi\rangle$ and all the interference terms $J_{\mu\nu}$ vanish. For example, for the lowest CMPC $|i_0\rangle$,

$$J^{(1)} = \frac{1}{\omega} \langle i_0 | J_z | i_0 \rangle = \frac{1}{\omega} \sum_{\mu(\text{occ. in } |i_0\rangle)} \langle \mu | j_z | \mu \rangle, \quad (10)$$

which, in general, is near the rigid-body value, but shows significant shell effects.

In [8,13] the PNC treatment was used to calculate the moments of inertia of the ND rare-earth nuclei. It was found that the experimentally observed bandhead moments of inertia of the ground bands in even-even nuclei and the odd-even differences in the bandhead moments of inertia can be reproduced very well by the PNC calculation, in which only the monopole pairing interaction is involved and the pairing interaction strength is determined by the observed odd-even mass differences. In [8,13], a CMPC truncation energy $E_c = 0.85\hbar\omega_0$ was adopted, and it was found the pairing interaction strength $G \approx 0.030\text{--}0.040 \hbar\omega_0$.

However, it has been noted that, although the smooth rise in the dynamic moment of inertia (of the SD bands in the $A = 190$ region) as a function of rotational frequency can be associated with the successive alignment of neutrons and protons in the presence of pairing interaction, the CSM calculations with monopole pairing interaction have not been able to reproduce both the low and high ω dependences of $J^{(2)}$ at the same time [28]. According to the CSM calculations for the SD bands in Hg nuclei [3,7,29], after the quasiparticle alignments have taken place $J^{(2)}$ will exhibit a downturn with increasing $\hbar\omega$ (at $\hbar\omega \sim 0.30$ MeV) towards the rigid-body value. Indeed, the decrease in $J^{(2)}$ (at $\hbar\omega \geq 0.4$ MeV) was recently observed in the yrast SD bands $^{194}\text{Hg}(1)$ [19] and $^{192}\text{Hg}(1)$ [5,16]. It is believed that to account for the evolution of $J^{(2)}$ with $\hbar\omega$ over the whole frequency range observed, particularly for the observed flattening of $J^{(2)}$ (at $\hbar\omega \geq 0.4$ MeV), the inclusion of quadrupole pairing seems necessary [28,30]. Our PNC calculation also confirmed the

downturn of $J^{(2)}$ near $\hbar\omega \sim 0.30$ MeV if only the monopole pairing interaction is involved in the CSM Hamiltonian (3), and in the calculation with both the monopole and quadrupole pairing interaction the postponement of the downturn of $J^{(2)}$ was found. However, the aim of the present paper is to compare the pairing interaction strength in SD and ND nuclei, we focus our attention to the difference in the moments of inertia at low frequency, particularly to the bandhead moment of inertia, in the following calculations only the monopole pairing interaction is involved. The problem of the evolution of $J^{(2)}$ with frequency is left to a separate paper [31], in which both the monopole and quadrupole pairing interactions are considered.

3.2 Calculated moments of inertia without pairing

It is well known, when the pairing correlation is neglected, the calculated moments of inertia are, in general, near the rigid-body value. However, the calculated moments of inertia show significant shell effect. For a closed shell configuration, $\langle J_z \rangle = 0$, so no contribution to the moment of inertia comes from a closed shell. For the SD nuclei near $A \approx 190$, no contribution comes from the neutrons and protons in the closed major shells, $N = 0, 1, 2, 3$. Calculation shows that for neutrons the main contributions come from the $N = 5, 6$ and 7 shells.

The cranked Nilsson orbits for neutrons in the vicinity of the Fermi surface of the SD Hg nuclei are displayed in Fig. 3, which is similar to the single-particle level schemes given by Bengtsson and Ragnarsson [32], Mayer et al. [33], and by Riley et al. [3] and Satula et al. [34] in a Woods-Saxon potential. Calculations show that the calculated moments of inertia depend closely on the CMPC, but do not depend sensitively on the detailed distribution of these orbits. Calculations using the Nilsson level scheme given by [32] were also made and the results are quite similar to the results given below. The calculated bandhead moments of inertia for the SD bands $^{192}\text{Hg}(1)$, $^{194}\text{Hg}(1)$ and $^{194}\text{Hg}(2,3)$ are given in Table 2, from which some features can be observed:

- (a) The contributions from the neutron $N = 5, 6$ and 7 shells are approximately 15–16%, 42–43%, and 41–42%, respectively. For $G_n = 0$, $N = 4$ shell is also closed and gives no contribution to the moments of inertia.
- (b) Though the calculated bandhead moments of inertia are similar for these SD bands, but there still exist small difference, i.e., the calculated $J_0(^{192}\text{Hg}(1)) > J_0(^{194}\text{Hg}(1)) > J(^{194}\text{Hg}(2,3))$, which is just *contrary* to the situation extracted from the phenomeno-

logical analysis.

- (c) The reason why $J_0(^{194}\text{Hg}(1)) < J_0(^{192}\text{Hg}(1))$ is the negative contribution to the moment of inertia from the two neutrons in ^{194}Hg occupying the highest neutron orbits $[512]5/2$ ($\alpha = \pm 1/2$) immediately below the Fermi surface. Similarly, due to the different negative contributions to the moments of inertia from the neutrons in the orbits $[512]5/2$ and $[624]9/2$, $|J_{\mu\mu}([624]9/2)| > |J_{\mu\mu}([512]5/2)|$ (see Table 1), we get $J_0(^{194}\text{Hg}([512]5/2 + [624]9/2)) < J_0(^{194}\text{Hg}(1))$.

The calculations without pairing shows that the difference in the moments of inertia is almost constant with rotational frequency. The calculated results for $G_n = 0$ are also displayed in Fig. 2; i.e., for $G_n = 0$

$$\delta J(^{194}\text{Hg}(2,3) - ^{192}\text{Hg}(1)) \approx -2.4\hbar^2\text{MeV}^{-1}$$

$$\delta J(^{194}\text{Hg}(2,3) - ^{194}\text{Hg}(1)) \approx -1.5\hbar^2\text{MeV}^{-1}$$

Therefore, merely to account for the observed difference in the moments of inertia for these SD bands at low frequency ($\hbar\omega \leq 0.2\text{ MeV}$), the inclusion of pairing interaction is absolutely necessary.

3.3 Influence of pairing interaction on the bandhead moments of inertia

Now we take into account the influence of pairing interaction on the moments of inertia. Because in this paper we focus our attention to the moments of inertia of SD bands at low frequency, we consider only the monopole pairing interaction. The calculated bandhead moments of inertia (in units of $\hbar^2\text{MeV}^{-1}$) of the SD bands in ^{194}Hg and their difference δJ_0 for various neutron pairing interaction strength G_n are as follows:

G_n ($\hbar\omega_{0n}$)	$J_n(^{194}\text{Hg}(1))$	$J_n(^{194}\text{Hg}(2,3))$	δJ_0
0	79.512	77.973	-1.539
0.005	76.231	75.554	-0.667
0.010	71.222	72.723	1.501
0.015	64.441	69.486	5.045
0.020	57.866	65.980	8.114
0.025	52.999	62.524	9.525
0.030	49.723	59.554	9.831

It is interesting to note that, though for $G_n = 0$ the calculated bandhead moments of inertia of $^{194}\text{Hg}(2,3)$ is smaller than that of $^{194}\text{Hg}(1)$, with increasing the pairing interaction

strength, $J_n(^{194}\text{Hg}(2,3))$ becomes gradually larger than $J_n(^{194}\text{Hg}(1))$. Here the blocking effect on the pairing plays an crucial role. PNC calculations show that increasing the pairing interaction strength will decrease the moments of inertia at low frequency. However, due to the blocking (anti-pairing) effect, the influence of pairing correlation on the moment of inertia is significantly reduced, i.e., the slope $|dJ_n/dG_n|$ for the two quasiparticle SD bands $^{194}\text{Hg}(2,3)$ is much smaller than for the quasiparticle vacuum band $^{194}\text{Hg}(1)$. It is seen that for the neutron pairing interaction strength $G_n = 0.015\hbar\omega_{0n}$, the calculated $\delta J_0 = J_n(^{194}\text{Hg}(2,3)) - J_n(^{194}\text{Hg}(1)) \approx 5.0\hbar^2\text{MeV}^{-1}$, is close to that extracted from the phenomenological analysis.

To illustrate the underlying microscopic mechanism, the contributions to the moments of inertia from each neutron major N shells ($N = 4, 5, 6, 7$) for $G_n = 0.015\hbar\omega_{0n}$ are given in Table 3. Comparing Tables 2 and 3, it is seen that when the pairing interaction is taken into account, the diagonal part, $\sum_{\mu} J_{\mu\mu}$, changes only a little, which can be understood from the slight change in the particle occupation due to pairing interaction [8]. For example, for $^{194}\text{Hg}(1)$, $\sum_{\mu} J_{\mu\mu} = 79.512$ (for $G_n = 0$) is changed to 78.577 (for $G_n = 0.015\hbar\omega_{0n}$), and for $^{194}\text{Hg}(2,3)$, $\sum_{\mu} J_{\mu\mu} = 77.973$ (for $G_n = 0$) is changed to 77.827 (for $G_n = 0.015\hbar\omega_{0n}$). However, when the pairing interaction is taken into account, a large number of CMPC's are mixed into the lowlying excited eigenstates of H_{CSM} , hence emerges the off-diagonal part $J_{\mu\nu}$ ($\mu \neq \nu$, see (9)), which, in general, is negative due to the destructive interference effects [8,13], so the calculated moment of inertia is significantly reduced. Physically, considering the anti-alignment effect of pairing interaction, this result is easily understandable. In particular, when μ and ν are the high- j intruder orbits near the Fermi surface, $|J_{\mu\nu}|$ is especially large (e.g., $\mu\nu = [770]1/2 [761]3/2; [761]3/2 [752]5/2; [633]7/2 [624]9/2; [640]1/2 [631]3/2; [642]3/2 [633]5/2; \text{etc.}$), and, in fact, the reduction of moments of inertia due to pairing correlation mainly comes from these orbits (for details, see the discussions in [8,13]. It has been well known that for normally deformed nuclei, the moments of inertia of the ground bands of even-even nuclei are reduced due to pairing correlation by a factor of about 1/2 (see [13]); i.e., the calculated bandhead moments of inertia with pairing is about one half of that without pairing. From the calculation given above, in contrast with the situation in ND nuclei, it is seen that,

$$J_n(^{192}\text{Hg}(1); G_n = 0.015\hbar\omega_{0n})/J_n(^{192}\text{Hg}(1); G_n = 0) = 79.4\%$$

$$J_n(^{194}\text{Hg}(1); G_n = 0.015\hbar\omega_{0n})/J_n(^{194}\text{Hg}(1); G_n = 0) = 81.0\%$$

i.e., the reduction of moments of inertia due to pairing correlation in SD nuclei is much smaller than in normally deformed nuclei. This may be considered as an indication that the pairing interaction strength in SD nuclei is much weaker than in ND nuclei. This reduction is even smaller for the two-quasiparticle SD band $^{192}\text{Hg}(2,3)$

$$J_n(^{194}\text{Hg}(2,3); G_n = 0.015\hbar\omega_{0n})/J_n(^{194}\text{Hg}(2,3); G_n = 0) = 89.1\%$$

which is understandable from the blocking effects on pairing correlation.

In fact, from the systematic analysis of the odd-even mass differences of the ND even-even rare-earth nuclei [13], it was found that the neutron pairing interaction strength in ND nuclei $G_n \sim 0.030\text{--}0.040 \hbar\omega_{0n}$ for $E_c = 0.85\hbar\omega_{0n}$. Therefore, we come to the conclusion that the neutron pairing interaction strength in the SD nuclei near $A = 190$ is about only one half of that in ND nuclei, i.e.,

$$G_n(\text{SD}) \sim \frac{1}{2}G_n(\text{ND}).$$

This result is consistent with the analysis for the $dJ^{(2)}/d\omega$, i.e., $|dJ^{(2)}/d\omega|$ is much steeper in the ND rare-earth and actinide nuclei than in the SD nuclei in the $A = 190$ region. In fact, the PNC calculation shows that decreasing the pairing interaction strength will increase the value of $J^{(2)}$ at low frequency and reduce the slope in $J^{(2)}$.

This work was supported by the National Science Foundation of China, and the Post-Doctorial Foundation of China.

References

- [1] E. F. Moore, et al., Phys. Rev. Lett. **63**, 360 (1989).
- [2] e.g., see R. V. F. Janssens, et al., Nucl. Phys. **A520**, 75c (1990); P. J. Twin, Nucl. Phys. **A520**, 17c (1990).
- [3] M. A. Riley, et al., Nucl. Phys. **A512**, 178 (1990).
- [4] D. Ye, et al., Phys. Rev. **C41**, R13 (1990).
- [5] P. Fallon, et al., Phys. Rev. **C51**, R1609 (1995).
- [6] F. S. Stephens, et al., Phys. Rev. Lett. **64**, 2623 (1990); **65**, 301 (1990).
- [7] R. R. Chasman, Phys. Lett. **B242**, 317 (1990).
- [8] J. Y. Zeng, Y. A. Lei, T. H. Jin and Z. J. Zhao, Phys. Rev. **C50**, 706 (1994).
- [9] Y. Liang, et al., Phys. Rev. **C46**, R2136 (1992).
- [10] J. R. Hughes, et al., Phys. Rev. **C51**, R447 (1995).
- [11] L. P. Farris, et al., Phys. Rev. **C51**, R2288 (1995).
- [12] D. J. Rowe, *Nuclear Collective Motion*, (Methuen, London, 1970), p. 194.
- [13] J. Y. Zeng, T. H. Jin and Z. J. Zhao, Phys. Rev. **C50**, 1388 (1994).
- [14] J. A. Becker, et al., Phys. Rev. **C41**, R9 (1990).
- [15] T. Lauritsen, et al., Phys. Lett. **B279**, 239 (1992).
- [16] B. J. P. Gall, et al., Z. Phys. **A347**, 223 (1994).
- [17] C. W. Beausang, et al., Z. Phys. **A335**, 325 (1990).
- [18] D. M. Cullen, et al., Nucl. Phys. **A520**, 105c (1990).
- [19] B. Cederwall, et al., Phys. Rev. Lett. **72**, 3150 (1994).
- [20] J. A. Becker, et al., Phys. Rev. **C46**, 889 (1992); Nucl. Phys. **A520**, 187c (1990).
- [21] J. E. Draper, et al., Phys. Rev. **C42**, R1791 (1990).
- [22] J. Y. Zeng, J. Meng, C. S. Wu, E. G. Zhao, Z. Xing and X. Q. Chen, Phys. Rev. **C44**, R1745 (1991); C. S. Wu, J. Y. Zeng, Z. Xing, X. Q. Chen and J. Meng, Phys. Rev. **C45**, 261 (1992).
- [23] R. Piepenbring and R. V. Protasov, Z. Phys. **A345**, 7 (1993).
- [24] e.g., C. L. Wu, D. H. Feng, and A. W. Guidry, Phys. Rev. Lett. **66**, 1377 (1991); R. A. Wyse and S. Pilotte, Phys. Rev. **C44**, R602 (1991).
- [25] H. X. Huang, C. S. Wu and J. Y. Zeng, Phys. Rev. **C39**, 1617 (1989).

- [26] P. Holmberg and P. O. Lipas, Nucl. Phys. A117, 552 (1968).
- [27] C. S. Wu and J. Y. Zeng, Commu. Theor. Phys. 8, 51 (1987).
- [28] I. Hamamoto and W. Nazarewicz, Phys. Rev. C49, 2489 (1994).
- [29] E. F. Moore, et al., Phys. Rev. Lett. 64, 3127 (1990).
- [30] W. Satula and W. Wyss, Phys. Rev. C50, 2888 (1994).
- [31] T. H. Jin, Y. A. Lei and J. Y. Zeng, to be submitted.
- [32] T. Bengtsson and I. Ragnarsson, Nucl. Phys. A436, 14 (1985).
- [33] M. Meyer, N. Redon, P. Quentin and J. Libert, Phys. Rev. C45, 233 (1992).
- [34] W. Satula, S. Cwiok, W. Nazarewicz, R. Wyss and A. Johnson, Nucl. Phys. A529, 289 (1991).

Table Captions

Table 1 Phenomenological analysis of the yrast SD bands $^{192}\text{Hg}(1)$, $^{194}\text{Hg}(1)$, and the excited signature partner SD bands $^{192}\text{Hg}(2,3)$ using (1). The spin assignments of these SD bands have been given in [2,4,6,17,18,20-23]. The values of a , b , c for each SD band are determined by the least squares fitting. χ is the relative root mean square deviation. $J_0 = \hbar^2/(ab + 2c)$ is the extracted bandhead moment of inertia.

Table 2 $J_{\mu\mu}$ (in units of $\hbar^2\text{MeV}^{-1}$) is the contribution to the moment of inertia from the neutron occupying the cranked Nilsson orbit μ , when the pairing interaction is neglected ($G_n = 0$). The contribution from a closed major shell is zero, $\sum_{\mu(\text{closed shell})} J_{\mu\mu} = 0$; i.e., for $G_n = 0$, all the contributions from the neutrons in the $N = 0, 1, 2, 3, 4$ shells vanish.

Table 3 The contributions to the moments of inertia (in units of $\hbar^2\text{MeV}^{-1}$) from neutrons in each major shell for the yrast SD bands $^{192}\text{Hg}(1)$, $^{194}\text{Hg}(1)$ and the two-quasiparticle SD bands $^{194}\text{Hg}([512]5/2 + [624]9/2)$. The pairing interaction strength $G_n = 0.015 \hbar\omega_{0n}$.

Table 1

I	¹⁹² Hg(1), α = 0		¹⁹⁴ Hg(1), α = 0		¹⁹⁴ Hg(2), α = 0		¹⁹⁴ Hg(3), α = 1	
	E _γ (I → I - 2), keV		E _γ (I → I - 2), keV		E _γ (I → I - 2), keV		E _γ (I + 1 → I - 1), keV	
	expt. [16]	calc.	expt. [17]	calc.	expt. [19]	calc.	expt. [19]	calc.
10	214.9	214.8			201.2	201.3		
12	258.2	258.1	254.3	254.3	242.6	242.7	262.6	262.6
14	300.4	300.5	296.2	296.4	283.5	283.5	303.0	303.1
16	341.7	341.8	337.7	337.6	323.8	323.8	342.9	342.9
18	382.0	382.2	377.8	377.8	363.5	363.4	382.1	382.0
20	421.2	421.4	417.1	416.9	402.4	402.3	420.4	420.0
22	459.5	459.6	455.2	455.1	440.5	440.4	458.3	458.1
24	496.8	496.7	492.3	492.2	477.9	477.8	495.1	495.0
26	532.8	532.9	528.3	528.2	514.5	514.3	531.2	531.1
28	568.0	568.1	563.6	563.3	550.0	550.1	566.3	566.4
30	602.5	602.4	597.3	597.4	585.0	585.0	601.2	601.0
32	636.1	635.9	630.5	630.6	619.1	619.1	635.2	634.9
34	669.0	668.7	662.4	662.9	652.1	652.4	667.5	668.0
36	700.9	700.7	693.8	694.3	684.8	684.8	700.0	700.4
38	732.2	732.1	725.4	725.0	716.2	716.5	731.9	732.1
40	762.8	762.9	754.6	754.9	747.4	747.5	763.2	763.2
42	793.0	793.1	783.9	784.1	777.5	777.6	793.5	793.6
44	822.5	822.8	812.9	812.7	807.6	807.1	823.9	823.5
46	852.1	852.1	841.0	840.7				
χ	3.17 × 10 ⁻⁴		4.19 × 10 ⁻⁴		2.75 × 10 ⁻⁴		3.49 × 10 ⁻⁴	
J ₀	86.99 (ħ ² MeV ⁻¹)		88.59 (ħ ² MeV ⁻¹)		93.56 (ħ ² MeV ⁻¹)		93.69 (ħ ² MeV ⁻¹)	
a	6.7141 × 10 ³ keV		1.0860 × 10 ⁴ keV		2.1358 × 10 ⁴ keV		1.4354 × 10 ⁵ keV	
b	8.1432 × 10 ⁻⁴		5.7960 × 10 ⁻⁴		3.1609 × 10 ⁻⁴		3.9473 × 10 ⁻⁴	
c	3.0140 keV		2.4983 keV		1.9685 keV		2.5038 keV	

Table 2

μ	¹⁹² Hg(1), α = 0		¹⁹⁴ Hg(1), α = 0		¹⁹⁴ Hg(2,3), α = 1	
	J _{μμ}		J _{μμ}		J _{μμ}	
	α = 1/2	α = -1/2	α = 1/2	α = -1/2	α = 1/2	α = -1/2
[550]1/2	-166.792	192.629	-166.787	192.639	-166.787	192.639
[541]3/2	-5.222	-3.999	-5.225	-4.003	-5.225	-4.003
[532]5/2	-2.261	-2.261	-2.263	-2.263	-2.263	-2.263
[541]1/2	51.193	-40.647	51.197	-40.643	51.197	-40.643
[523]7/2	-1.872	-1.872	-1.873	-1.873	-1.873	-1.873
[530]1/2	-21.073	26.473	-21.072	26.475	-21.072	26.475
[521]3/2	0.353	0.357	0.353	0.357	0.353	0.357
[532]3/2	-1.596	-1.881	-1.597	-1.883	-1.597	-1.883
[514]9/2	-1.638	-1.638	-1.639	-1.640	-1.639	-1.640
[523]5/2	-1.487	-1.487	-1.488	-1.488	-1.488	-1.488
[521]1/2	34.345	-33.545	34.346	-33.545	34.346	-33.545
[505]11/2	-1.464	-1.464	-1.465	-1.465	-1.465	-1.465
[512]5/2			-0.442	-0.442	-0.442	
Σ _μ J _{μμ} (N = 5)	13.148		12.274		12.716	
[660]1/2	218.437	-184.446	218.447	-184.432	218.447	-184.432
[651]3/2	-3.966	-5.792	-3.966	-5.797	-3.966	-5.797
[642]5/2	-2.658	-2.658	-2.660	-2.660	-2.660	-2.660
[651]1/2	13.677	0.509	13.682	0.515	13.682	0.515
[633]7/2	-2.123	-2.123	-2.125	-2.124	-2.125	-2.124
[640]1/2	-10.018	14.055	-10.017	14.057	-10.017	14.057
[642]3/2	0.611	0.810	0.611	0.811	0.611	0.811
[624]9/2					-1.981	
Σ _μ J _{μμ} (N = 6)	34.317		34.342		32.361	
[770]1/2	-202.804	249.477	-202.784	249.493	-202.784	249.493
[761]3/2	-8.457	-5.346	-8.464	-5.349	-8.464	-5.349
Σ _μ J _{μμ} (N = 7)	32.870		32.896		32.896	
J _n	80.335		79.512		77.973	

Table 3

(a) $^{192}\text{Hg}(1)$

N	$\sum_{\mu} J_{\mu\mu}$	$\sum_{\mu<\nu} J_{\mu\nu}$	sum
4	0.0123	-0.0022	0.0101
5	12.9445	-1.0152	11.9293
6	33.5722	-5.4663	28.1059
7	33.1878	-9.4508	23.737
all shells	79.7168	-15.9345	63.782

(b) $^{194}\text{Hg}(1)$

N	$\sum_{\mu} J_{\mu\mu}$	$\sum_{\mu<\nu} J_{\mu\nu}$	sum
4	0.0084	-0.0013	0.0071
5	12.2392	-1.0811	11.1581
6	33.4884	-5.0137	28.4747
7	32.8410	-8.0405	24.8005
all shells	78.577	-14.1366	64.441

(c) $^{194}\text{Hg} ([512]5/2 + [624]9/2)$

N	$\sum_{\mu} J_{\mu\mu}$	$\sum_{\mu<\nu} J_{\mu\nu}$	sum
4	0.0024	-0.0002	0.0022
5	12.6553	-0.2511	12.4042
6	32.3093	-2.1573	30.1520
7	32.8598	-5.9325	26.9273
all shells	77.8268	-8.3411	69.486

Figure Captions

Fig. 1 The ω variation of the moments of inertia for the SD bands $^{192}\text{Hg}(1)$ and $^{194}\text{Hg}(1,2,3)$.

The dynamic and kinematic moments of inertia extracted by using (2) are denoted by dotted lines for $^{192}\text{Hg}(1)$ and solid lines for $^{194}\text{Hg}(1,2,3)$. The $J^{(2)}$ extracted by using $J^{(2)} = 4\hbar^2/\Delta E_{\gamma}$ is denoted by open triangle for $^{192}\text{Hg}(1)$ and solid triangle for $^{194}\text{Hg}(1,2,3)$. The $J^{(1)}$ extracted by using $J^{(1)} = (2I-1)\hbar^2/E_{\gamma}(I \rightarrow I-2)$ is denoted by open circle for $^{192}\text{Hg}(1)$ and solid circle for $^{194}\text{Hg}(1,2,3)$.

Fig. 2 The ω variation of the extracted difference in the kinematic and dynamic moments of inertia. (a) $J(^{194}\text{Hg}(2,3)) - J(^{192}\text{Hg}(1))$; (b) $J(^{194}\text{Hg}(2,3)) - J(^{194}\text{Hg}(1))$.

Fig. 3 The cranked Nilsson neutron orbits in the vicinity of the Fermi surface of the SD Hg nuclei. The Nilsson parameters for the neutron orbits are $\epsilon_2 = 0.45$, $\epsilon_4 = 0.024$, $\gamma = 0$, and $\kappa = 0.068, 0.072, 0.068, 0.065$ and $\mu = 0.390, 0.440, 0.350, 0.300$ for $N = 4, 5, 6, 7$ shell respectively.

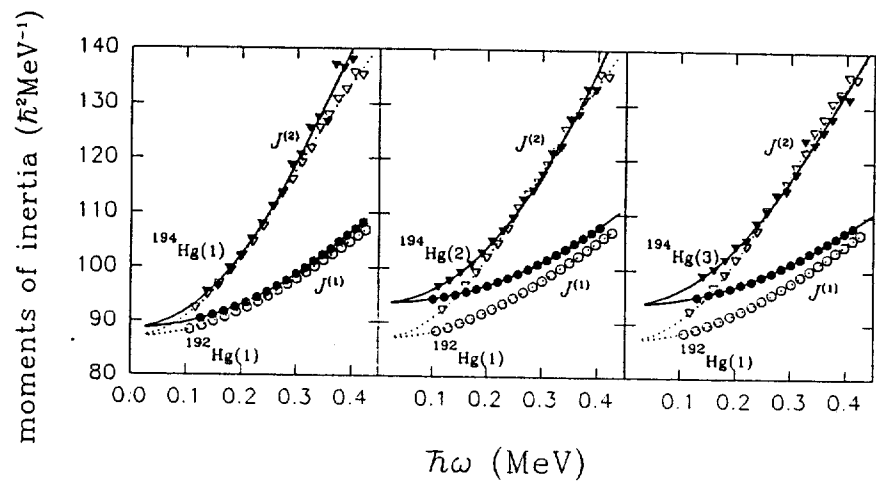


Fig. 1

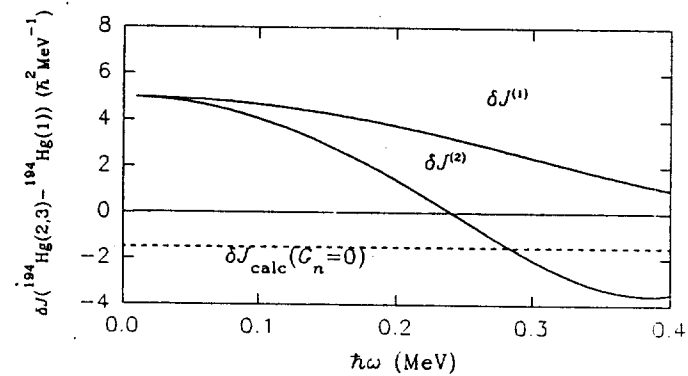


Fig. 2b

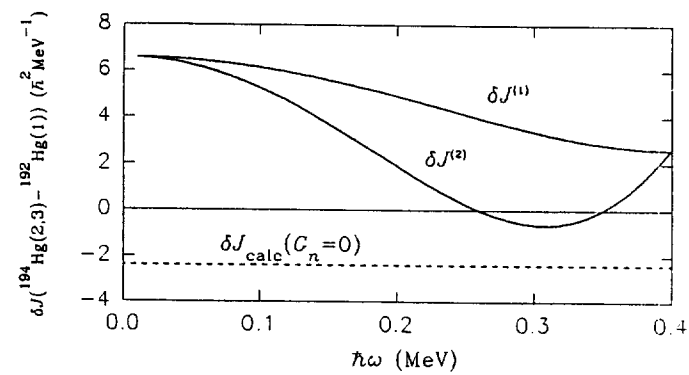


Fig. 2a

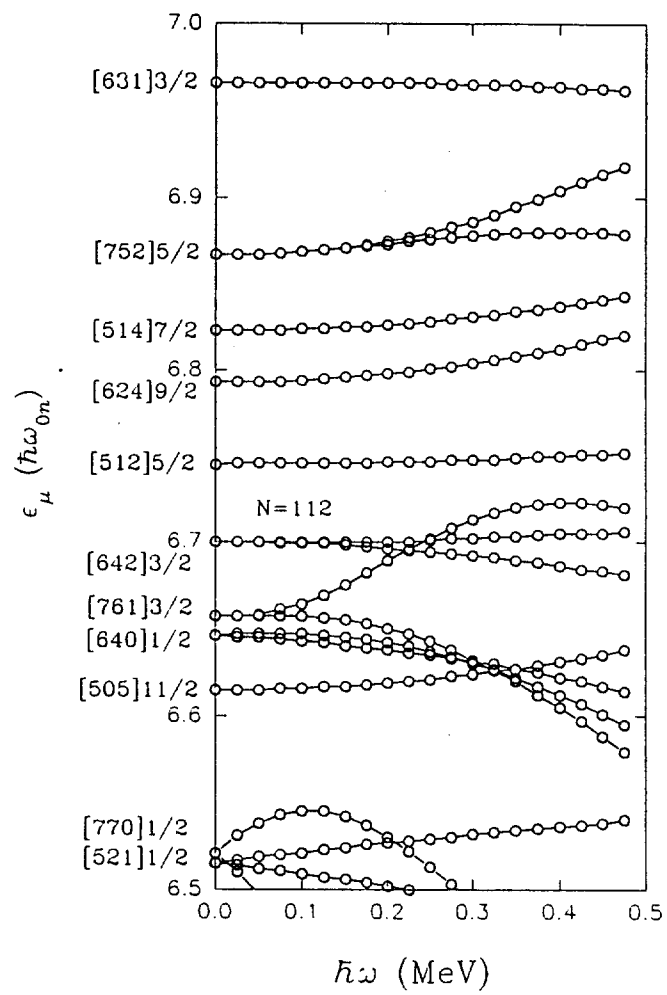


Fig. 3